

Persistence of pinning and creep beyond critical drive within the strong pinning paradigm

M. Buchacek¹, R. Willa^{1,2}, V.B. Geshkenbein¹, and G. Blatter¹

¹*Institute for Theoretical Physics, ETH Zurich, 8093 Zurich, Switzerland and*

²*Materials Science Division, Argonne National Laboratory, Lemont, IL 60439, USA*

(Dated: August 7, 2018)

Pinning and thermal creep determine the response of numerous systems containing superstructures, e.g., vortices in type II superconductors, domain walls in ferroics, or dislocations in metals. The combination of drive and thermal fluctuations lead to the superstructure's depinning and its velocity v determines the electric, magnetic, or mechanical response. It is commonly believed that pinning and creep collapse above the critical drive F_c , entailing a sharp rise in the velocity v . We challenge this perception by studying the effects of thermal fluctuations within the framework of strong vortex pinning in type-II superconductors. In fact, we show that pinning and thermal creep persist far beyond the critical force. The resulting force-velocity characteristic largely maintains its zero-temperature shape and thermal creep manifests itself by a downward renormalisation of the critical drive. Such characteristics is in agreement with Coulomb's law of dry friction and has been often observed in experiments.

I. INTRODUCTION

The phenomenological behavior of numerous technological materials is determined by topological defects, well known examples being vortices in superconductors^{1,2}, dislocations in metals^{3,4}, or domain walls in ferroic materials^{5,6}. Driving these topological objects via suitable forces induces motion, with dramatic consequences for the material's properties, e.g., loss of dissipation-free current transport in superconductors, appearance of plastic flow in metals, or loss of magnetic coercivity in a ferromagnet. Material imperfections come to rescue by pinning these topological defects, vortices, dislocations, or domain walls, at least up to a critical drive F_c where pinning is finally overcome. Common perception then tells that depinning, helped by thermal fluctuations, is a dramatic effect that induces a steep onset of the superstructure's motion and a rapid collapse of rigidity. In this paper, we demonstrate that such common expectation is not generally applicable: assuming a strong pinning scenario^{8,9} applied to vortices in type II superconductors with a small density of defects¹⁰, we demonstrate that pinning and thermal creep persist far beyond the critical drive, leading to a linear excess-current characteristic that is shifted by the action of thermal fluctuations.

Given the ubiquitousness of the phenomenon, studies of the onset of motion of pinned objects encompass a wide spectrum. A simple but instructive setup is given by a particle sliding down a tilted washboard potential. This model describes the depinning of the superconducting phase and incipient voltage in a current-driven Josephson junction^{11–13} and has been used to describe the motion of flux bundles in a pinning potential^{14,15}: at depinning, the particle dissipatively starts moving down the tilted washboard potential and the velocity rises steeply, $v \propto (F - F_c)^{1/2}$, as pinning collapses beyond F_c . Effects of thermal creep then are essentially limited to drives $F < F_c$ below critical, see Fig. 1(a). Dynamical char-

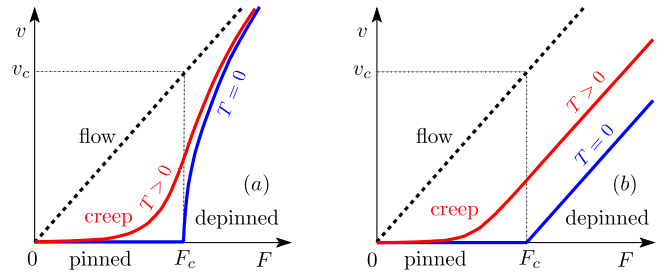


FIG. 1. Velocity–force characteristics of a bulk superconductor: (a) common perception with pinning force collapsing above F_c , (b) calculated excess-force characteristic in accord with Coulomb's law; $v_c = F_c/\eta$ denotes the velocity for free dissipative motion at F_c . Thermal creep appears mainly below F_c in (a), while the persistence of pinning beyond F_c in (b) allows creep to manifest beyond F_c .

acteristics with steep velocity-onset as illustrated in Fig. 1(a) have become a common perception in drawing the shape of a velocity–force characteristic, e.g., of superconducting material^{2,7,16,17}. In a similar vein, effects of thermal creep are expected to manifest at drives $F < F_c$.

However, this view contrasts with (classic) experimental data on bulk superconducting material^{18,19} and recent theoretical analysis²⁰ where the non-linear dynamical response assumes the shape of an excess-force characteristic, see Fig. 1(b). This different shape is in agreement with Coulomb's law of dry friction, telling that the static- and dynamical pinning forces are equal and hence the pinning force persists even at drives beyond critical, $F > F_c$. Using strong pinning theory, we show that thermal effects produce a downward shift of the critical- (or depinning-) force-density, while preserving the shape of the excess-force characteristic, see Figs. 1(b) and 3, confirming the presence of pinning and its thermal reduction at large drives $F > F_c$.

II. STRONG PINNING THEORY

We consider a vortex lattice with density $a_0^{-2} = B/\Phi_0$, $\Phi_0 = hc/2e$ the flux unit, induced by a field B directed along the z -axis. A current density j along y drives these flux lines via the Lorentz-force density $F_L = jB/c$ along x . Their free dissipative motion $v = F_L/\eta$, η the viscosity²¹, is hugely modified by pinning due to material defects, see Fig. 1. Here, we use strong pinning theory^{8,9} in combination with Kramer's rate theory²² to determine the mean pinning-force density $\langle F_{\text{pin}}(v, T) \rangle$ opposing the vortex motion and study its dependence on the creep velocity v and temperature T . Using the result for $\langle F_{\text{pin}}(v, T) \rangle$ in the vortex dynamical equation

$$\eta v = F_L(j) - \langle F_{\text{pin}}(v, T) \rangle, \quad (1)$$

we find the material's velocity-current (v - j) characteristic at finite temperatures T and evaluate the current-dependent barriers governing vortex creep.

For a small pin density n_p and defects that pin no more than one vortex, the pinning problem can be reduced^{8-10,23} to an effective single-pin-single-vortex setup. The latter involves a defect with a potential $e_p(\mathbf{R})\delta(z)$ of depth e_p and extension ξ , the coherence length, that we place at the origin. The vortex features an effective elasticity $\bar{C} \sim \sqrt{\varepsilon_0 \varepsilon_l}/a_0$, where $\varepsilon_l = \varepsilon_0 \ln(a_0/\xi)$ and $\varepsilon_0 = (\Phi_0/4\pi\lambda)^2$ denote the vortex line elasticity and line energy, respectively, and λ is the screening length. With \bar{C} related to the local static elastic Green's function of the vortex lattice, we account for the elastic forces of neighboring vortices^{8-10,23}. Assuming defects of intermediate strength with $e_p/\xi < \varepsilon_0$ guarantees the applicability of elasticity theory²⁴. Given an asymptotic position ρ at large values of $|z|$, the vortex is locally distorted by the presence of the defect, what results in a deformation \mathbf{u} within the plane $z = 0$. For a radially symmetric potential $e_p(R)$, the problem further reduces to a scalar one involving only the radial asymptotic distance ρ of the vortex from the pin and the vortex displacement u pointing towards the pin, hence $u < 0$. The radial position $\rho + u$ of the vortex tip can be found by minimizing the sum of pinning- and elastic energies, see Fig. 2,

$$e_{\text{pin}}(u; \rho) = e_p(\rho + u) + \bar{C}u^2/2 \quad (2)$$

at fixed asymptotic position ρ , $\partial_u e_{\text{pin}}(u; \rho) = 0$, and we obtain the self-consistency equation for $u(\rho)$,

$$\bar{C}u(\rho) = f_p[\rho + u(\rho)], \quad (3)$$

with $f_p(R) = -\partial_R e_p(R)$ the defect's force profile. On the other hand, the total derivative

$$-\frac{de_{\text{pin}}[u(\rho); \rho]}{d\rho} = f_p[\rho + u(\rho)] \equiv f_{\text{pin}}(\rho) \quad (4)$$

provides us with the effective pinning force.

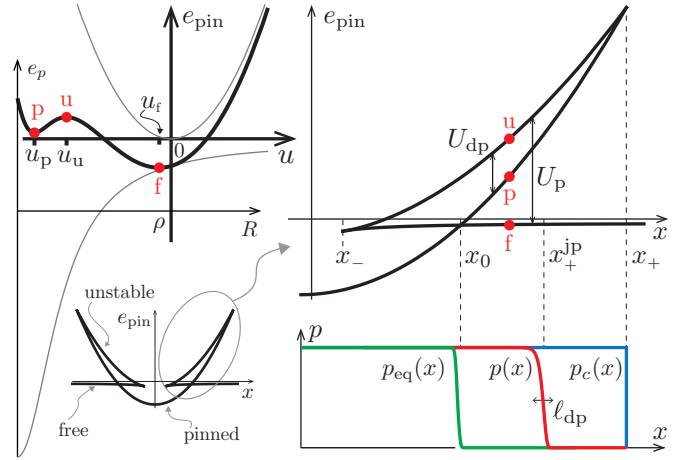


FIG. 2. Top left: energy landscape $e_{\text{pin}}(u; \rho)$ versus u (thick lines) as well as pinning potential $e_p(R)$ versus R and elastic energy $\bar{C}u^2/2$ (thin lines). Shown is a situation for $x_- < x < x_+$ with two local minima, pinned and free, with large and small distortions $u_p < 0$ and $u_f < 0$. The unstable solution at u_{u} defines the barrier separating the two minima. The bottom sketch shows the pinning landscape $e_{\text{pin}}(x)$ for a vortex driven along the x -axis with free, pinned, and unstable branches at different asymptotic positions x . Top right: expanded view of the region $x_- < x < x_+$ with barriers $U_{\text{dp}}(x)$ and $U_{\text{p}}(x)$ for depinning (vanishing $\propto (x_+ - x)^{3/2}$ at x_+) and pinning (vanishing at x_-); the maximal barrier U_0 is attained at the branch crossing point x_0 . Bottom right: branch occupation $p(x; v, t)$ at $T = 0$ and $v = 0$ ($\rightarrow p_c$), at finite T and v ($\rightarrow p$), and at equilibrium ($\rightarrow p_{\text{eq}}$).

In the weak pinning situation, where the elasticity dominates, the nonlinear self-consistency equation (3) has a unique solution and pinning is collective, involving many competing defects. Strong pinning appears when the Labusch parameter $\kappa \equiv \max_R[\partial_R f_p(R)]/\bar{C}$ is pushed beyond unity, $\kappa > 1$. The total energy $e_{\text{pin}}(\rho) \equiv e_{\text{pin}}[u(\rho); \rho]$ then exhibits multiple minima associated with pinned $[u_p(\rho)]$ and free $[u_f(\rho)]$ vortex configurations at the same asymptotic position ρ , see Fig. 2. Here, we consider strong pins with $\kappa > 1$ in the presence of a small defect density with $n_p < (a_0 \xi^2 \kappa)^{-1}$, implying less than one active pin per volume a_0^3 —these conditions delineate the three-dimensional strong-pinning regime in the n_p - f_p diagram of Ref. [10].

A current density j along y pushes the vortices along x and we can reduce the problem to a one-dimensional geometry. The pinning-force density $\langle F_{\text{pin}}(v, T) \rangle$ depends on the occupation probability $p(x; v, T)$ of the pinned branch (the force along y averages to 0),

$$\langle F_{\text{pin}} \rangle = -n_p \frac{2t_{\perp}}{a_0} \int \frac{dx}{a_0} [p f_{\text{pin}}^{\text{p}}(x) + (1-p) f_{\text{pin}}^{\text{f}}(x)], \quad (5)$$

where $f_{\text{pin}}^{\text{f,p}}(x) \equiv f_p[x + u_{\text{f,p}}(x)]$ are the effective pinning forces generated by the free and pinned branches and the integral is limited to the interval $[-a_0/2, a_0/2]$ due to the periodicity of the lattice. At small density n_p ,

different defects do not interact and thus $\langle F_{\text{pin}} \rangle \propto n_p$; furthermore, the average over y can be included with a factor $2t_{\perp}/a_0$, where t_{\perp} denotes the distance along y over which vortices get trapped²⁴. At $T = 0$ and in the pinned state with $v = 0$, the maximally asymmetric occupation $p_c = \chi(-x_-, x_+)$ determines the critical force density $F_c = \langle F_{\text{pin}}(0, 0) \rangle$, where $\chi(a, b)$ denotes the characteristic function on the interval $[a, b]$ and $\pm x_{\pm}$ are the boundaries of the pinned and free branches; the condition $e_p/\xi < \varepsilon_0$ implies that $x_+ < a_0$ and the periodicity of the vortex lattice does not interfere with the pinning process. Evaluating the integral in (5) with the help of (4), we obtain the critical force density

$$F_c = (2x_-/a_0) n_p [\Delta e_p + \Delta e_{\text{dp}}]/a_0 \quad (6)$$

with the jumps in energy $\Delta e_p = [e_{\text{pin}}^f - e_{\text{pin}}^p]_{x=-x_-}$ upon pinning at $-x_-$, $\Delta e_{\text{dp}} = [e_{\text{pin}}^p - e_{\text{pin}}^f]_{x=x_+}$ at depinning, and $e_{\text{pin}}^{f,p}(x) \equiv e_{\text{pin}}[u_{f,p}(x); x]$. For a radially symmetric pinning potential, vortices approaching the defect jump into the pin at a distance $\rho = x_-$ and hence the transverse trapping length is given by $t_{\perp} = x_-$.

III. THERMAL FLUCTUATIONS

At finite temperatures $T > 0$, inspired by the work on charge-density-wave pinning^{25,26}, see also Ref.²⁷, we can find the branch occupation probability $p(x; v, T)$ within the bistable regions $x_- < |x| < x_+$ from the rate equation (note that $p(|x| > x_+) = 0$ and $p(|x| < x_-) = 1$)

$$\partial_t p = v \partial_x p = -p \omega_p e^{-U_{\text{dp}}/T} + (1-p) \omega_f e^{-U_p/T}. \quad (7)$$

The barriers $U_{p,\text{dp}}$ are determined by the third solution $u_{\text{ii}}(x)$ of Eq. (3) which is unstable, see Fig. 2, $U_p(x) = e_{\text{pin}}^u(x) - e_{\text{pin}}^p(x)$ and $U_{\text{dp}}(x) = e_{\text{pin}}^u(x) - e_{\text{pin}}^f(x)$. The attempt frequencies $\omega_{p,f}(x)$ relate to the curvatures of the total energy $e_{\text{pin}}(u; x)$ at the extremal points and account for the dissipative vortex dynamics²².

A. Large drives

For *large drives* $F_L \sim F_c$, the occupation probability $p(x; v, T)$ maintains its steps, albeit smoothed due to thermal fluctuations and shifted to new positions $x_{\pm}^{\text{jp}}(v, T)$ where vortices jump between free and pinned branches, see Fig. 2. In determining the depinning point $x_+^{\text{jp}}(v, T) < x_+$, we focus on the first term in Eq. (7). We define the local relaxation length $\ell_{\text{dp}}(x) \equiv [v/\omega_p(x)] e^{U_{\text{dp}}(x)/T}$ and take another derivative of Eq. (7) to obtain the curvature $\partial_x^2 p \approx (p/\ell_{\text{dp}}^2)(1 + \ell'_{\text{dp}})$. We define the jump position through the inflection point, i.e., $\partial_x^2 p(x_{\pm}^{\text{jp}}) = 0$, and arrive at the condition $\ell_{\text{dp}}(x_{\pm}^{\text{jp}}) \approx T/|U'_{\text{dp}}(x_{\pm}^{\text{jp}})|$ for x_{\pm}^{jp} , with $f'(x)$ the derivative of $f(x)$

and we have ignored the x -dependence of ω_p . The criterion for the pinning point $-x_-^{\text{jp}}$ is derived from an analogous consideration with $\ell_p = (v/\omega_f) e^{U_p/T}$ replacing ℓ_{dp} . Defining the thermal velocity scale²⁸

$$v_{\text{th}} = \omega_p T / |U'_{\text{dp}}(x_+^{\text{jp}})| \sim \kappa^s \omega_f T / |U'_p(x_-^{\text{jp}})| \quad (8)$$

with $s = (n+3)/(n+2)$ depending on the decay $e_p(x) \propto x^{-n}$, we can cast these criteria into the simple form

$$U_{\text{dp}}(x_+^{\text{jp}}) \approx U_p(x_-^{\text{jp}}) \approx T \ln(v_{\text{th}}/v). \quad (9)$$

These results are valid for barriers $U_{\text{dp},p} \gg T$, i.e., for velocities v small compared to v_{th} . As v approaches v_{th} at large drives $F_L > F_c$, $x_{\pm}^{\text{jp}} \rightarrow x_{\pm}$, the barriers $U_{\text{dp},p}$ vanish, and the characteristic approaches the $T = 0$ result.

B. Small drives

At *small drives*, the jump locations x_{\pm}^{jp} approach the branch crossing point x_0 where the barrier $U_0 = U_{\text{dp}}(x_0) = U_p(x_0)$ is maximal, see Fig. 2. Pinning and depinning transitions become equally important and the probability $p(x; v, T)$ differs perturbatively from the equilibrium occupation $p_{\text{eq}}(x) = [1 + \ell_p(x)/\ell_{\text{dp}}(x)]^{-1}$. The rate equation (7) can be rewritten in the form $\partial_x p = (p_{\text{eq}} - p)/\ell_{\text{eq}}$, with the equilibrium relaxation length $\ell_{\text{eq}}(x)$ given by $\ell_{\text{eq}}^{-1} = \ell_p^{-1} + \ell_{\text{dp}}^{-1}$; its solution takes the form of a right-shifted equilibrium occupation, $p(x) \approx p_{\text{eq}}[x - \ell_{\text{eq}}(x)]$.

IV. RESPONSE CHARACTERISTIC

The branch occupation probabilities $p(x; v, T)$ determine the effective pinning-force density via Eq. (5). In addition, for small creep velocities, we have $t_{\perp}(v, T) = x_{\pm}^{\text{jp}}$, with a saturation at x_0 as $v \rightarrow 0$. Finally, the velocity v is found from a self-consistent solution of the vortex equation of motion (1). Below, we carry out this program and determine the superconductor's v - j characteristic that is shown Fig. 3.

A. Large drives

We first consider large drives $F_L \sim F_c$. Given the small width $\ell_{\text{dp}} \sim (T/e_p) x_+$ of the jump in the occupation probability $p(x; v, T)$, see Fig. 2, we can use the approximation $p(x; v, T) \approx \chi(-x_-^{\text{jp}}, x_+^{\text{jp}})$ in Eq. (5) and obtain the pinning-force density

$$\langle F_{\text{pin}}(v, T) \rangle = (2x_-^{\text{jp}}/a_0) n_p [\Delta e_p^{\text{jp}} + \Delta e_{\text{dp}}^{\text{jp}}]/a_0 \quad (10)$$

with the reduced jumps Δe_p^{jp} and $\Delta e_{\text{dp}}^{\text{jp}}$ evaluated at the positions $x = -x_-^{\text{jp}}$ and $x = x_+^{\text{jp}}$, cf. Eq. (6). Expanding

Eq. (10) for small deviations $\delta x_{\pm} = \pm(x_{\pm} - x_{\pm}^{\text{jp}}) > 0$ and normalizing, we obtain the force-density ratio

$$\frac{\langle F_{\text{pin}}(v, T) \rangle}{F_c} = 1 + \frac{\delta x_-}{x_-} - \frac{\Delta e'_p \delta x_- + \Delta e'_{\text{dp}} \delta x_+}{\Delta e_p + \Delta e_{\text{dp}}}, \quad (11)$$

where $\Delta e'_p$ and $\Delta e'_{\text{dp}}$ denote derivatives of Δe_p and Δe_{dp} at $-x_-$ and x_+ , respectively. The first (positive, since $x_-^{\text{jp}} > x_-$) correction is due to the change in the trapping distance t_{\perp} , while the second term represents the decrease in the pinning-force density due to the reduced asymmetry in the branch occupation. Assuming a smooth pinning potential $e_p(x)$ of depth e_p and large κ , one finds³⁰ that $U_{\text{dp}}(x_+^{\text{jp}}) \sim e_p(\delta x_+/\kappa\xi)^{3/2}$ and $U_p(x_-^{\text{jp}}) \sim e_p\kappa^s(\delta x_-/\kappa\xi)^{3/2}$. Using these results with $U_p \approx U_{\text{dp}}$ in Eq. (11), we find that

$$\langle F_{\text{pin}}(v, T) \rangle / F_c \approx 1 - g(\kappa)(U_{\text{dp}}/e_p)^{2/3}, \quad (12)$$

with $g(\kappa) = \tilde{g}(\kappa)[\kappa/(\kappa - 1)]^{4/3}$ collecting all prefactors of δx_{\pm} and $\tilde{g}(\kappa)$ depending on the shape of $e_p(x)$, $\tilde{g}(\kappa)$ of order 2 for a Lorentzian shaped potential³⁰ $e_p(R) = e_p/(1 + R^2/2\xi^2)$. Combining this result with Eq. (9), the equation of motion (1) assumes the simple form

$$v/v_c = j/j_c - 1 + g(\kappa)(T/e_p)^{2/3} [\ln(v_{\text{th}}/v)]^{2/3} \quad (13)$$

that involves the critical current density $j_c = cF_c/B$ and two velocity scales, the flux-flow velocity at F_c , $v_c = F_c/\eta \propto n_p$, and the thermal velocity v_{th} , see Eq. (8). The v - j characteristic is easily obtained by plotting $j(v)$, see Fig. 3. At $T = 0$, we recover the linear excess-current characteristic²⁰ with $v = v_c(j/j_c - 1)$ for current densities $j > j_c$. The effect of thermal fluctuations is conveniently analyzed via the differential resistivity scaled with the free flux-flow resistivity $\rho_{\text{ff}} \propto v_c/j_c$,

$$\frac{\rho_d}{\rho_{\text{ff}}} \equiv \frac{d(v/v_c)}{d(j/j_c)} = \left[1 + \frac{2\tau^{2/3}}{3} \frac{v_c/v}{[\ln(v_{\text{th}}/v)]^{1/3}} \right]^{-1}, \quad (14)$$

where we have defined the rescaled temperature $\tau = g^{3/2}(\kappa)T/e_p$. As illustrated in Fig. 3, ρ_d expressed through j assumes a step-like form that is shifted to lower currents as T increases. We define the depinning current-density $j_{\text{dp}}(T)$ through the inflection point $\partial_j^2 \rho_d = 0$; assuming a large ratio $\alpha = (v_{\text{th}}/v_c)\tau^{-2/3}$, we find that

$$j_{\text{dp}}(T) \approx j_c [1 - \tau^{2/3} \{\ln[3\alpha(\ln 3\alpha)^{1/3}]\}^{2/3}] \quad (15)$$

and $\rho_d(j_{\text{dp}}) \approx \rho_{\text{ff}}/3$. The velocity ratio $v_{\text{th}}/v_c = (T/e_p)a(\kappa)/n_p a_0 \xi^2$ involves another factor $a(\kappa) = \tilde{a}(\kappa)\kappa^{-1/(n+2)}[\kappa/(\kappa - 1)]^{3/2}$ that depends on $e_p(x)$, with $\tilde{a}(\kappa)$ of order 0.1 for a Lorentzian potential³⁰.

The rounding of the v - j characteristic near j_{dp} is conveniently described by a creep barrier $U(j) \equiv U_{\text{dp}}[v(j), T]$; approximating the equation of motion (1) $\langle F_{\text{pin}} \rangle / F_c \approx j/j_c$ for small velocities v and using (12), we find a creep-type motion $v \approx v_{\text{th}} e^{-U(j)/T}$ with a barrier

$$U(j \lesssim j_c) \approx e_p [(1 - j/j_c)/g(\kappa)]^{3/2}. \quad (16)$$

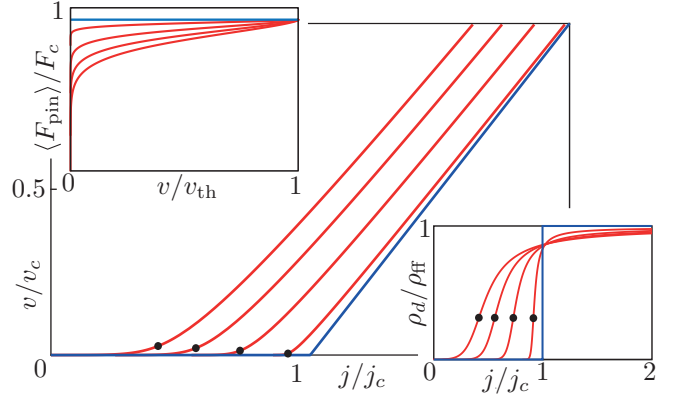


FIG. 3. v - j characteristic at temperatures $T/e_p = (0, 0.1, 0.5, 1.0, 1.5) \times 10^{-2}$ and for a small defect density $n_p a_0 \xi^2 = 10^{-4}$; we have chosen a Labusch parameter $\kappa = 5$ implying $g(\kappa) \approx 2.8$ and $a(\kappa) \approx 0.17$ for a Lorentzian potential $e_p(R)$. Thermal fluctuations lead to a downward shift of j_c to $j_{\text{dp}}(T)$, with the latter (solid points) defined through the inflection point in $\rho_d(j)$, see lower-right inset. The weak logarithmic dependence on v of ρ_d at currents $j > j_c$ closely preserves the shape of the excess-current characteristic also at finite T , with creep manifesting itself well above j_c . The top-left inset shows the pinning-force density $\langle F_{\text{pin}}(v, T > 0) \rangle / F_c$, reduced due to thermal creep for velocities $v < v_{\text{th}}$. Linear TAFF response is not visible on this scale.

The most important feature of the v - j characteristic in Fig. 3 is the persistence of creep far beyond j_c . This is very different from a characteristic describing a rapid collapse of the pinning-force density beyond j_c with a steep rise in velocity v at j_c and thermal creep prevailing below j_c , see Fig. 1(a). For strongly-pinned vortices, the pinning-force density $\langle F_{\text{pin}}(v) \rangle$ persists for drives beyond j_c ; such behavior coincides with Coulomb's law of dry friction that is at the origin of the excess-current characteristic²⁰. Since $\langle F_{\text{pin}}(v) \rangle$ survives j_c , depinned vortices still profit from thermal activation and creep manifests itself beyond j_c . Furthermore, changes in the pinning-force density $\langle F_{\text{pin}}(v) \rangle$ are logarithmic in v and hence small, giving rise to a flat resistivity $\rho_d(j)$ above j_c . As a result, the v - j characteristic is renormalized downwards but keeps an excess-current form at finite temperatures, see Fig. 3. Finally, the characteristic joins the $T = 0$ excess-current characteristic at $j_{\text{th}} = j_c(1 + v_{\text{th}}/v_c)$ where $x_{\pm}^{\text{jp}} \rightarrow x_{\pm}$ and the pinning-force density $\langle F_{\text{pin}}(v_{\text{th}}) \rangle = F_c$, see Fig. 3, with the velocity ratio $v_{\text{th}}/v_c \propto T/n_p$ attaining large values for small defect densities n_p .

B. Small drives

We find the pinning-force density $\langle F_{\text{pin}}(v, T) \rangle$ at small velocities $v \lesssim v_{\text{TAF}} = v_{\text{th}} e^{-U_0/T}$ (i.e., small drives $F_L \ll F_c$) by inserting the shifted equilibrium distribution $p_{\text{eq}}[x - \ell_{\text{eq}}(x)]$ into Eq. (5). Expanding in small

$\ell_{\text{eq}} \propto v$ and making use of the anti-symmetry $f_{\text{pin}}^{\text{p,f}}(x) = -f_{\text{pin}}^{\text{p,f}}(-x)$, we obtain

$$\langle F_{\text{pin}} \rangle \approx -n_p \frac{2x_0}{a_0} \int \frac{dx}{a_0} \ell_{\text{eq}}(x) p'_{\text{eq}}(x) \Delta f_{\text{pin}}(x) \quad (17)$$

with $\Delta f_{\text{pin}}(x) = f_{\text{pin}}^{\text{f}}(x) - f_{\text{pin}}^{\text{p}}(x)$. A simple estimate is obtained by replacing $p'_{\text{eq}}(x)$ with a sum of δ -functions at $\pm x_0$, see Fig. 2; accounting for the precise shapes of $p_{\text{eq}}(x)$ and $\ell_{\text{eq}}(x)$ contributes a κ -dependent prefactor. Using $\ell_{\text{eq}}(x_0) = v(\omega_p + \omega_f)^{-1} e^{U_0/T}$ and the scalings $\omega_{\text{p,f}} \sim (e_p/\xi^2)/\eta a_0^3$, $x_0 \sim \xi$, and $\Delta f_{\text{pin}}(x_0) \sim e_p/\xi$, we arrive at the result

$$\langle F_{\text{pin}}(v, T) \rangle = \eta v h(\kappa) (n_p a_0 \xi^2) e^{U_0/T}, \quad (18)$$

with the barrier $U_0 = e_p \tilde{u}(\kappa) [(\kappa - 1)/\kappa]^2$ and all κ -dependence absorbed in $h(\kappa) = \tilde{h}(\kappa) \kappa^{(n+2)/(4n+4)} [\kappa/(\kappa-1)]^{1/2}$; for a Lorentzian potential, we find $\tilde{h}(\kappa)$ of order 20 and $\tilde{u}(\kappa)$ of order 0.3 (for $\kappa = 5$, we have $h(\kappa) \approx 36$ and $U_0/e_p \approx 0.18$). At low temperatures, Eq. (18) implies a TAFF characteristic with an exponentially suppressed slope as compared to free flux-flow,

$$\frac{v}{v_c} = \frac{j}{j_c} \frac{e^{-U_0/T}}{h(\kappa) n_p a_0 \xi^2}. \quad (19)$$

The crossover to the non-linear characteristic is realized at the velocity v_{TAFF} corresponding to the driving current $j_{\text{TAFF}} \approx a(\kappa) h(\kappa) (T/e_p) j_c$.

V. CONCLUSION

In conclusion, we have shown that, contrary to usual expectation, thermal creep persists far beyond the critical depinning current density j_c when pins are dilute and strong. This unexpected result is in accord with the excess-current characteristic following from Coulomb's law. Such a characteristic and its temperature dependence is easily set apart from the steep characteristic associated with the collapse of the pinning force beyond j_c , possibly due to the avalanche-type depinning conjectured for weakly-pinned random elastic manifolds^{16,31}. These insights provoke further work directed at understanding the crossover between the dry-friction type characteristic typical for diluted strong pins and the collapse-type characteristic usually associated with dense weak pins. Finally, strong pinning theory provides a quantitative result for the linear TAFF response at small currents, see Eq. (19). The latter has been experimentally observed and quantitatively analyzed, e.g., in high temperature superconductors³²⁻³⁴; conversely, the downward shift and rounding of the excess-current characteristic predicted by strong pinning theory awaits more detailed experimental and numerical investigations.

ACKNOWLEDGMENTS

We thank A.E. Koshelev for discussions and acknowledge financial support from the Swiss National Science Foundation through the Division II, the National Centre of Competence in Research 'MaNEP-Materials with Novel Electronic Properties' and an Early Postdoc.Mobility Fellowship (R.W.). The work at Argonne was supported by the US Department of Energy, Office of Science, Materials Sciences and Engineering Division.

¹ G. Blatter, M.V. Feigelman, V.B. Geshkenbein, A.I. Larkin, and V.M. Vinokur, Rev. Mod. Phys. **66**, 1125 (1994).
² E.H. Brandt, Rep. Prog. Phys. **58**, 1465 (1995).
³ M.E. Kassner, Fundamentals of Creep in Metals and Alloys (Elsevier Science & Technology Books, Amsterdam, 2015).
⁴ C. Zhou, C. Reichhardt, C.J. Olson, J. Reichhardt, and I.J. Beyerlein, Scientific Reports **5**, 8000 (2015).
⁵ W. Kleemann, Annu. Rev. Mater. Res. **37**, 415 (2007).
⁶ J. Gorchon, S. Bustingorry, J. Ferré, V. Jeudy, A.B. Kolton, and T. Giamarchi, Phys. Rev. Lett. **113**, 027205 (2014).
⁷ T. Nattermann and S. Scheidl, Adv. Phys. **49**, 607 (2000).
⁸ R. Labusch, Cryst. Lattice Defects **1**, 1 (1969).
⁹ A.I. Larkin and Y.N. Ovchinnikov, J. Low Temp. Phys. **34**, 409 (1979).
¹⁰ G. Blatter, V.B. Geshkenbein, and J.A.G. Koopmann, Phys. Rev. Lett. **92**, 067009 (2004).
¹¹ L.G. Aslamazov and A.I. Larkin, JETP Lett. **9**, 87 (1969).

¹² V. Ambegaokar and B.I. Halperin, Phys. Rev. Lett. **22**, 1364 (1969).
¹³ M. Tinkham, *Introduction to Superconductivity* (Dover Publications Inc., New York, 2004).
¹⁴ A. Schmid and W. Hauger, J. Low Temp. Phys. **11**, 667 (1973).
¹⁵ D.R. Tilley and J. Tilley, *Superfluidity and Superconductivity* (IOP Publishing Ltd., Philadelphia, 1990).
¹⁶ P. Chauve, T. Giamarchi, and P. Le Doussal, Phys. Rev. B **62**, 6241 (2000).
¹⁷ T. Giamarchi, A. Kolton, A. Rosso, Dynamics of Disordered Elastic Systems, in: M.C. Miguel, M. Rubi (eds) Jamming, Yielding, and Irreversible Deformation in Condensed Matter. Lecture Notes in Physics, vol 688 (Springer, Berlin, Heidelberg, 2006).
¹⁸ A.R. Strnad, C.F. Hempstead, and Y.B. Kim, Phys. Rev. Lett. **13**, 794 (1964); Y.B. Kim, C.F. Hempstead, and A.R. Strnad, Phys. Rev. **139**, A1163 (1965).
¹⁹ Z.L. Xiao and E.Y. Andrei, Y. Paltiel, E. Zeldov, P. Shuk, and M. Greenblatt, Phys. Rev. B **65**, 094511 (2002).

- ²⁰ A.U. Thomann, V.B. Geshkenbein, and G. Blatter, Phys. Rev. Lett. **108**, 217001 (2012).
- ²¹ J. Bardeen and M. J. Stephen, Phys. Rev. **140**, A1197 (1965).
- ²² H. Kramers, Physica **7**, 284 (1940).
- ²³ R. Willa, V.B. Geshkenbein, and G. Blatter, Phys. Rev. B **93**, 064515 (2016).
- ²⁴ A.U. Thomann, V.B. Geshkenbein, and G. Blatter, Phys. Rev. B **96**, 144516 (2017).
- ²⁵ S. Brazovskii and A. Larkin, J. Phys. IV France **9**, 177 (1999).
- ²⁶ S. Brazovskii and T. Nattermann, Adv. Phys. **53**, 177 (2004).
- ²⁷ D.S. Fisher, Phys. Rev. B **31**, 1396 (1985).
- ²⁸ Close to x_+ the velocity scale v_{th} assumes a constant value $v_{\text{th}} = (\kappa_+/2\pi)(T/\eta a_0^3 \xi)$ with $\kappa_+ = \xi f_p''[x_+ + u_p(x_+)]/2\bar{C} \sim \kappa$, where the last relation is valid for very strong pinning.
- ²⁹ P.H. Kes, J. Aarts, J. van den Berg, J. van der Beek, and J.A. Mydosh, Supercond. Sci. Technol. **1** 242 (1989).
- ³⁰ M. Buchacek, R. Willa, V.B. Geshkenbein, and G. Blatter (unpublished).
- ³¹ O. Narayan and D.S. Fisher, Phys. Rev. B **46** 11520 (1992).
- ³² Y. Iye, T. Tamegai, H. Takeya, H. Takei, Jpn. J. Appl. Phys. **26**, L1057 (1987).
- ³³ T.T.M. Palstra, B. Batlogg, L.F. Schneemeyer, and J.V. Waszczak, Phys. Rev. Lett. **61**, 1662 (1988).
- ³⁴ M. Tinkham, Phys. Rev. Lett. **61**, 1658 (1988).